(a) **PNS v. 1.0.0 beta**
Parameter definition list updated at 15-10-2012
Usage: only txt file sequence.
The txt file must contain only 'g','c','a','t' or 'u' (small) character to specify the nucleotides of the sequence.

Result of the elaboration of file : C:\TEMP\EUROPA.TXT

Sequence loaded!
244 nucleotides loaded in memory.

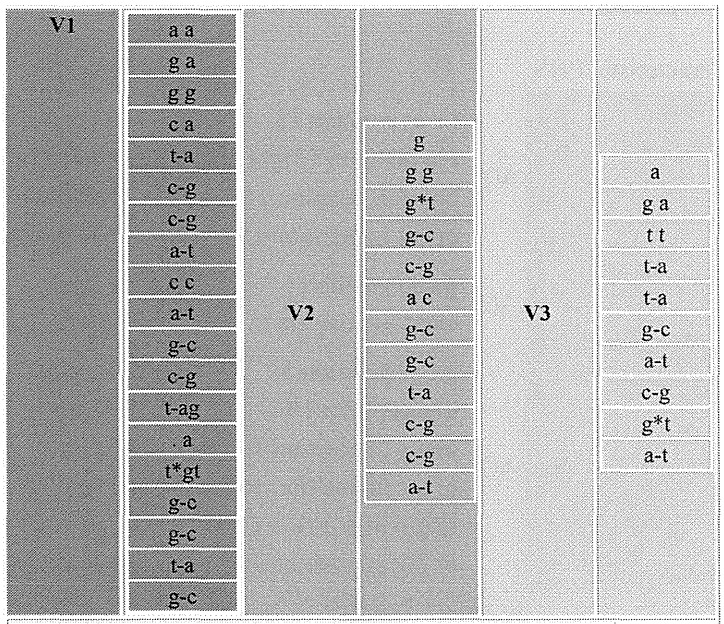

Genus characteristic PNS: PNS recognized.		
V1:	t in position 22	There is no binding to check.
	t in position 5 right nucleotide	YES (t*gt)
	c c in position 11	YES (c c)
	a t in position 10	YES (a-t)
	c g in position 8	YES (c-g)
	or t a in position 8	NO (c-g)
	or t g in position 8	NO (c-g)
	or g g in position 8	NO (c-g)
	t a in position 7	YES (t-a)
	or a a in position 7	NO (t-a)
	or g c in position 7	NO (t-a)
	. a in position 6	YES (. a)

Fig. 3. Result .html type file of genotyping according to the PNS method of the Europa Strain (accession number AB000898). The 5′-UTR sequence was compared to known *Pestivirus* species BVDV-1, BVDV-2, BDV, CSFV and the new proposed taxons. The three palindromic regions in sequences were identified in the sequence and shown in the first part of the file. Genus *Pestivirus* characteristic PNS and BVDV-1 species characteristic PNS were identified in the palindromes and highlighted in the following section of the file. Genotyping was completed using BVDV-1c specific PNS.

showed possible combinations of G/A/CnAC and CUnG/A which were consecutive in the sequence. In the CSFV strains Alfort and Brescia, starting from the V2, reading back for the V1 identification, with the first CUnG/A sequence G in position 217 and the following first G/A/CnAC sequence with C in position 210, the program, without correct parameters, constructed a very short V1 (not shown). The correct combination was obtained with the G/A/CnAC sequence in position 194. Similar aspects were observed in the BVD-2a strains 713/2, 11mi97 and 552195 and BVDV-1b Influenza2.

In case of an incomplete V1 sequences, as for BVDV-1 strains Massimo 1, 2 and 4, the V1 palindrome was constructed according to a predicted structure corresponding to the conserved locus in the genus. The program completed the construction of the V2 and V3 palindromes and the related genotyping procedure. The genus and species characteristics were determined. The identified genotype specific PNS were not sufficient to allocate these strains. In the case of the V1 sequence being absent, as for BVDV-1 strain M98, BVDV-2 strains 59386 and Scp, and BDV strain L83/I84, the program was arranged to determine species and genotype specific PNS in the remaining two loci, V2 and V3. For example, in strain M98 sequence the program could identify the BVDV-1 species specific PNS G-C in position 5 in V2 and in V3.

The PNS software represents a transition in the *Pestivirus* genetic characterization method by using a computerized procedure,

(b)

	or . g in position 6	NO (. a)
	t g in position 5	YES (t*g)
	g c in position 4	YES (g-c)
V2:	g t in position 10	YES (g*t)
	or g c in position 10	NO (g*t)
	c g in position 8	YES (c-g)
	or t g in position 8	NO (c-g)

Species characteristic PNS:

BVDV-1: PNS recognized.	V1:	t a in position 15	YES (t-a)
		t in position 5 right nucleotide	YES (t*gt)
		or t g in position 15	NO (t-a)
		or c g in position 15	NO (t-a)
	V2:	g c in position 5	YES (g-c)
		or a t in position 5	NO (g-c)
	V3:	g c in position 5	YES (g-c)
		a in position 10	YES (a)
		or a a in position 10	NO (a)
		or a c in position 10	NO (a)
		or g a in position 10	NO (a)
		or g c in position 10	NO (a)

Genotype characteristic PNS:

BVDV-1c: PNS recognized.	V1:	c g in position 14	YES (c-g)
		or c a in position 14	NO (c-g)
	V2:	a c in position 7	YES (a c)
	V3:	a t in position 4	YES (a-t)

Fig. 3. (*Continued*).

which is an improvement, with the main advantage being the rapid testing procedure and provision of data for accurate analyses. The prototype of the program demonstrated it to be a simple and useful tool for the sequence testing, giving clear results for the allocation of unknown isolates and providing support for research work through identification of unusual characteristics in strategic genomic regions. In addition to the recognized PNS, all structures with similarity or divergence, in terms of specific nucleotide base pairings in the virus genomic sequences at the 5′-UTR level with possible expression of evolutionary changes or virus biological activities, such as virulence (Topliff and Kelling, 1998) were made available.

The software for the PNS method we have developed and presented here is called PNS and is available free at www.pns-software.com. This full computerization of the procedure eliminates the main limitation of manual searching of relevant base pairings and direct observation of the sequence. It has simplified the genotyping procedure with easy access for the users and gives rapid testing with reliable results. It takes into account the secondary structures predicted at the three variable regions in the 5′-UTR for the classification of *Pestivirus*. Future improvements will be required to further standardize the procedure and increase the performance of the software to eliminate any possible incoherence. This aspect could also be important for possible future adaptation of the methodology to other positive polarity RNA virus species.

Acknowledgements

We extend our thanks to Dr. Roger D. Ayling, Mycoplasma Group, Department of Bacteriology, Animal health and Veterinary Laboratories Agency, Addlestone, Surrey, United Kingdom, who kindly helped us in the realization of this study.

References

Apicella, C., Thesis of Doctorate 1999. Una Metodologia per la Progettazione ad Oggetti di Applicazioni Relazionali: Moduli Back-end. University of Salerno, Italy.

Deng, R., Brock, K.V., 1993. 5′ and 3′ untranslated regions of pestivirus genome: primary and secondary structure analyses. Nucleic Acids Res. 21, 1949–1957.

Ellis, M.A., Stroustrup, B., 1990. The Annotated C++ Reference Manual. Editors Addison Wesley, London.

Freier, S.M., Kierzek, R., Jaeger, J.A., et al., 1986. Improved free-energy parameters for predictions of RNA duplex stability, 83. Proc. Natl. Acad. Sci., USA, pp. 9373–9377.

Giangaspero, M., 2011. Genetic variation of border disease virus species strains. Vet. Italiana 47, 415–435.

Giangaspero, M., Harasawa, R., 2011. Classification of *Pestivirus* species genotypes based on palindromic nucleotide substitutions, a genetic marker in the 5′ untranslated region of genomic RNA. J. Virol. Methods 174, 166–172.

Giangaspero, M., Harasawa, R., 2008. Genetic variation of classical swine fever virus based on palindromic nucleotide substitutions, a genetic marker in the 5′ untranslated region of RNA. Vet. Italiana 44, 305–318.

Giangaspero, M., Harasawa, R., Weber, E.L., Belloli, A., 2008. Genoepidemiological evaluation of Bovine viral diarrhea virus 2 species based on secondary structures in the 5′ genomic untranslated region. J. Vet. Med. Sci. 70, 571–580.

Giangaspero, M., Vacirca, G., Harasawa, R., Büttner, M., Panuccio, A., De Giuli Morghen, C., Zanetti, A., Belloli, A., Verhulst, A., 2001. Genotypes of *Pestivirus* RNA detected in live virus vaccines for human use. J. Vet. Med. Sci. 63, 723–733.

Harasawa, R., 1994. Comparative analysis of the 5′ non-coding region of pestivirus RNA detected from live virus vaccines. J. Vet. Med. Sci. 56, 961–964.

Harasawa, R., Giangaspero, M., 1998. A novel method for pestivirus genotyping based on palindromic nucleotide substitutions in the 5′-untranslated region. J. Virol. Methods 70, 225–230.

Harasawa, R., Giangaspero, M., Ibata, G., Paton, D.J., 2000. Giraffe strain of pestivirus Its taxonomic status based on the 5′ untranslated region. Microbiol. Immunol. 44, 915–921.

King, A.M.Q., Adams, M.J., Carstens, E.B., Lefkowitz, E.J., 2012. Virus Taxonomy. Ninth Report of the International Committee on Taxonomy of Viruses. Elsevier-Academic Press, Amsterdam.

Kirkland, P.D., Frost, M.J., Finlaison, D.S., King, K.R., Ridpath, J.F., Gu, X., 2007. Identification of a novel virus in pigs-Bungowannah virus: a possible new species of pestivirus. Virus Res. 129, 26–33.

Lodi, E., Pacini, G., 1998. In: Bollati Boringhieri (Ed.), Introduzione alle Strutture di dati. BOLLATI G. BORINGHIERI P., Bologna, Italy.

Thompson, J.D., Gibson, T.J., Plewniak, F., Jaenmougin, F., Higgins, D.G., 1997. The CLUSTAL X windows interface: flexible strategies for multiple sequence alignment aided by quality analysis tools. Nucleic Acids Res. 25, 4867–4882.

Topliff, C.L., Kelling, C.L., 1998. Virulence markers in the 5′ untranslated region of genotype 2 bovine viral diarrhea virus isolates. Virology 250, 164–172.

Vilček, S., Ridpath, J.F., Van Campen, H., Cavender, J.L., Warg, J., 2005. Characterization of a novel pestivirus originating from a Pronghorn antilope. Virus Res. 108, 187–193.

Zuker, M., Stiegler, P., 1981. Optimal computer folding of large RNA sequences using thermodynamics and auxiliary. Nucleic Acids Res. 9, 133–148.

NOTE *Bacteriology*

Two Genotypes among '*Candidatus* Mycoplasma haemobos' Strains Based on the 16S-23S rRNA Intergenic Spacer Sequences

Fumina SASAOKA[1)], Jin SUZUKI[1)], Yusaku WATANABE[1,4)], Masatoshi FUJIHARA[1,4)], Kazuya NAGAI[2)], Toh-ichi HIRATA[3)] and Ryô HARASAWA[1,4)]*

[1)]*Department of Veterinary Microbiology, Faculty of Agriculture, Iwate University, Morioka 020–8550, Japan*
[2)]*Cryobiofrontier Research Center, Faculty of Agriculture, Iwate University, Morioka 020–8550, Japan*
[3)]*Omyojin Research Farm, Faculty of Agriculture, Iwate University, Morioka 020–8550, Japan*
[4)]*The United Graduate School of Veterinary Science, Gifu University, Gifu 501–1193, Japan*

(Received 6 August 2012/Accepted 1 October 2012/Published online in J-STAGE 15 October 2012)

ABSTRACT. '*Candidatus* Mycoplasma haemobos', sometimes causative of bovine infectious anemia at various extents, has been demonstrated throughout the world. Here, we show two distinct types of '*Ca.* M. haemobos' are distributed among cattle in Japan, by examining the primary and secondary structures of the 16S-23S rRNA intergenic spacer region that has been shown to be a stable genetic marker for mycoplasma species. Our results may explain differences in severity of anemic condition as well as provide a genetic marker for an epidemiological study of bovine hemoplasma infections.
KEYWORDS: hemoplasma, mycoplasma, rRNA.

doi: 10.1292/jvms.12-0349; *J. Vet. Med. Sci.* 75(3): 361–364, 2013

'*Candidatus* Mycoplasma haemobos (synonym of '*Ca.* M. haemobovis')' is a trivial name of hemotropic mycoplasma that may cause anemia at various degrees in cattle [11, 12, 16, 18]. Reason of different severity in anemic condition caused by '*Ca.* M. haemobos' infection has yet been unknown. Although this alleged species has provisionally been identified by only nucleotide sequence of the 16S rRNA gene because of uncultivable trait [10, 17, 20], genetic variation in this species remained unexplored. In our previous study, the 16S-23S rRNA intergenic spacer (ITS) region of hemoplasma was found to be a useful tool for determination of taxonomic status of this particular species [15] as well as other mycoplasma species [2, 4–6]. Here, we show the '*Ca.* M. haemobos' strains are divided into two distinct types according to the ITS sequences.

EDTA-anticoagulated blood samples were collected from 25 Japanese black cattle bred on an experimental farm at Omyojin (latitude 39.7N and longitude 141.1E) of Iwate University during October 2011 to March 2012. Total DNA was extracted from 200 μl of the whole blood samples by using the QIAamp DNA Blood Mini Kit (QIAGEN, Hilden, Germany) according to the manufacturer's instructions, eluting into 200 μl of buffer AE, and stored at −20°C until examination in the PCR assay. No clinical symptom was reported on the cattle examined, despite infection by *Bovine leukemia virus*.

Hemoplasma infection was found in all the 25 cattle diagnosed by real-time PCR by using forward primer Hemo-F1, 5′-ATATTCCTACGGGAAGCAGC-3′, equivalent to nucleotide numbers 328 to 347 of *M. wenyonii* and reverse primer Hemo-R1, 5′-ACCGCAGCTGCTGGCACATA-3′, equivalent to nucleotide numbers 503 to 522 of *M. wenyonii* as described previously [13]. Real-time PCR was performed in a SmartCycler instrument (Cepheid, Sunnyvale, CA, U.S.A.) with SYBR Premix Ex *Taq*(Code #RR041A, TaKaRa Bio., Otsu, Japan). The reaction mixture contained 1 μl of each primer (10 pmol/μl), 12.5 μl of 2X premix reaction buffer and water to volume of 23 μl. Finally, 2 μl of DNA samples as templates were added to this mixture. Amplification was carried out 40 cycles of denaturation at 95°C for 5 sec, renaturation at 57°C for 20 sec and elongation at 72°C for 15 sec, after the initial denaturation at 94°C for 30 sec. After real-time PCR, melting experiment was performed from 60 to 95°C at 0.2°C/sec with smooth curve setting averaging one point. Melting peaks were visualized by plotting the first derivative against the melting temperature as described previously [7].

Of all the cattle examined, eight cattle were found infected with '*Ca.* M. haemobos' alone based on the 16S rRNA gene analysis, and they were subjected to analysis of the ITS region by end-point PCR. Briefly, PCR amplification was carried out at 94°C for 30 sec, 55°C for 2 min and 72°C for 2 min for 30 cycles using forward (5′-GTTCCCAGGTCTTGTACACA-3′) and reverse (5′-CAGTACTTGTTCACTATCGGTA-3′) primers as described previously [1]. The PCR products were then fractionated on horizontal, submerged 1.0% SeaKem ME agarose gels (FMC Bioproducts, Rockland, ME, U.S.A.) in TAE (40 mM Tris, pH8.0, 5 mM sodium acetate and 1 mM disodium ethylenediaminetetra cetate) buffer at 50 volts for 60 min. After electrophoresis, the gels were stained in ethidium bromide solution (0.4 $\mu g/ml$) for

*CORRESPONDENCE TO: HARASAWA, R, Department of Veterinary Microbiology, Faculty of Agriculture, Iwate University, Morioka 020–8550, Japan.
e-mail: harasawa-tky@umin.ac.jp

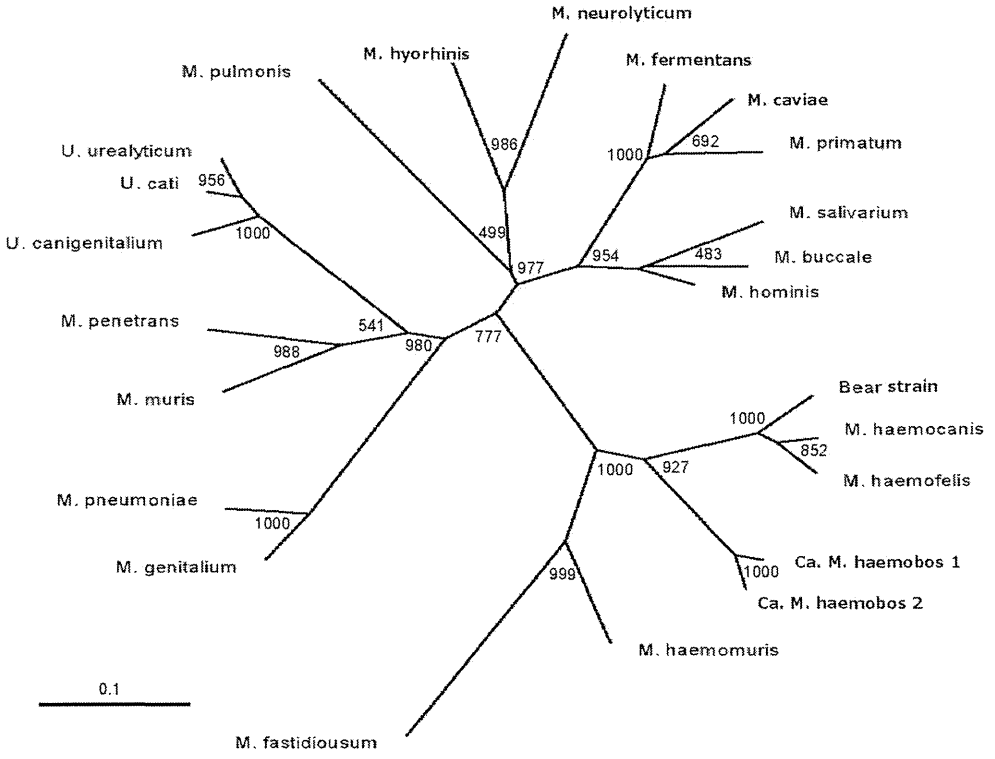

Fig. 1. Unrooted phylogenetic tree based on the ITS comparison, suggesting a monophyletic relationship among hemoplasmas and *M. fastidiosum*. Following nucleotide sequences obtained from the DNA databases are shown with an accession number in parenthesis. They are *M. salivarium* PG20 (X58558), *M. pulmonis* m53 (X58554), *M. neurolyticum* Sabin Type A (X58552), *M. buccale* CH20247 (D89504), *M. primatum* HRC292 (D89509), *M. caviae* G122 (D89505), *M. hominis* PG21 (X58559), *M. fermentans* PG18 (X58553), *M. hyorhinis* BTS-7 (X58555), *M. penetrans* GTU54 (D89508), *M. muris* RIII4 (D89507), *M. pneumoniae* Mac (D14528), *M. genitalium* G37 (D14526), *M. fastidiosum* ATCC33229 (AY781782), *Ureaplasma urealyticum* T960 (X58561), *U. cati* F2 (D636859, *U. canigenitalium* D6P-C (D63684), *M. haemomuris* Shizuoka (AB080799), *M. haemofelis* Gandai2 (AB638408), Bear hemoplasma strain (AB725596), '*Ca.* M. haemobos' typel Gandai1 (AB638407) and '*Ca.* M. haemobos' type 2 B2.20 (AB740010). Scale bar indicates the estimated evolutionary distance that was computed with CLUSTAL W [19] using neighbor-joining method [14]. Numbers in the relevant branches refer to the values of boot-strap probability of 1,000 replications.

15 min and visualized under UV transilluminator. DNA in a clearly visible band was extracted by using NucleoSpin Extract II kit (Macherey-Nagel, Düren, Germany) and was subjected to direct sequencing in a 3500 Genetic Analyzer (Applied Biosystems, Foster City, CA, U.S.A.). The GenBank/EMBL/DDBJ accession numbers for ITS sequences of '*Ca.* M. haemobos' strains used in this study are AB740009 through AB740016.

The nucleotide sequences of ITS regions of the '*Ca.* M. haemobos' strains were compared with authentic mycoplasma species in phylogenetic analysis. In the present study, we examined the phylogenetic relatedness among 23 mycoplasma species including not only 3 ureaplasmas but also 6 hemoplasmas, *M. haemomuris*, *M. haemofelis*, '*Ca.* M. haemominutum', bear strain and 2 types of '*Ca.* M. haemobos' (Fig. 1). In addition to our previous illustration of ITS from '*Ca.* M. haemobos' type 1 [15], the present analysis revealed existence of another type of ITS among '*Ca.* M. haemobos' strains. Alignment of nucleotide sequences of ITS regions defined so far indicated 94% similarity between these two genotypes (Table 1). Of the eight strains, six were identical to the '*Ca.* M. haemobos' type 1, and the remaining two strains showed an identical but were distinct from type 1 sequence. Although we examined only Japanese black cattle without clinical symptom, this variation can be used for an epidemiological marker of '*Ca.* M. haemobos' infections in cattle population, since nucleotide sequences in ITS region have been conserved within a mycoplasma species or subspecies [2, 6, 8].

The secondary structures of the ITS were predicted according to the algorithm of Zuker and Stiegler [21]. Five stem-loop domains were allocated in ITS of '*Ca.* M. haemobos' (Fig. 2). Domains III and V were well conservative, despite several deletions in others domains. Secondary structures in ITS region have sometime provided a key character to distinguish closely related species of mycoplasmas [3, 6, 7, 9]. In the present study, ITS regions of the two genotypes of '*Ca.* M. haemobos' showed characteristic features of myco-

Table 1. Similarity matrix showing nucleotide sequence homology among the ITS regions of hemoplasmas. Nucleotide sequences of ITS regions have been determined on only four species. Numbers indicate homology percentage between two ITS sequences.

	M. haemocanis	*M. haemofelis*	Bear strain	*Ca.* M. haemobos 1	*Ca.* M. haemobos 2	*M. haemomuris*
M. haemocanis	100					
M. haemofelis	95	100				
Bear strain	93	93	100			
Ca. M. haemobos 1	80	81	81	100		
Ca. M. haemobos 2	82	82	83	94	100	
M. haemomuris	44	44	44	43	44	100

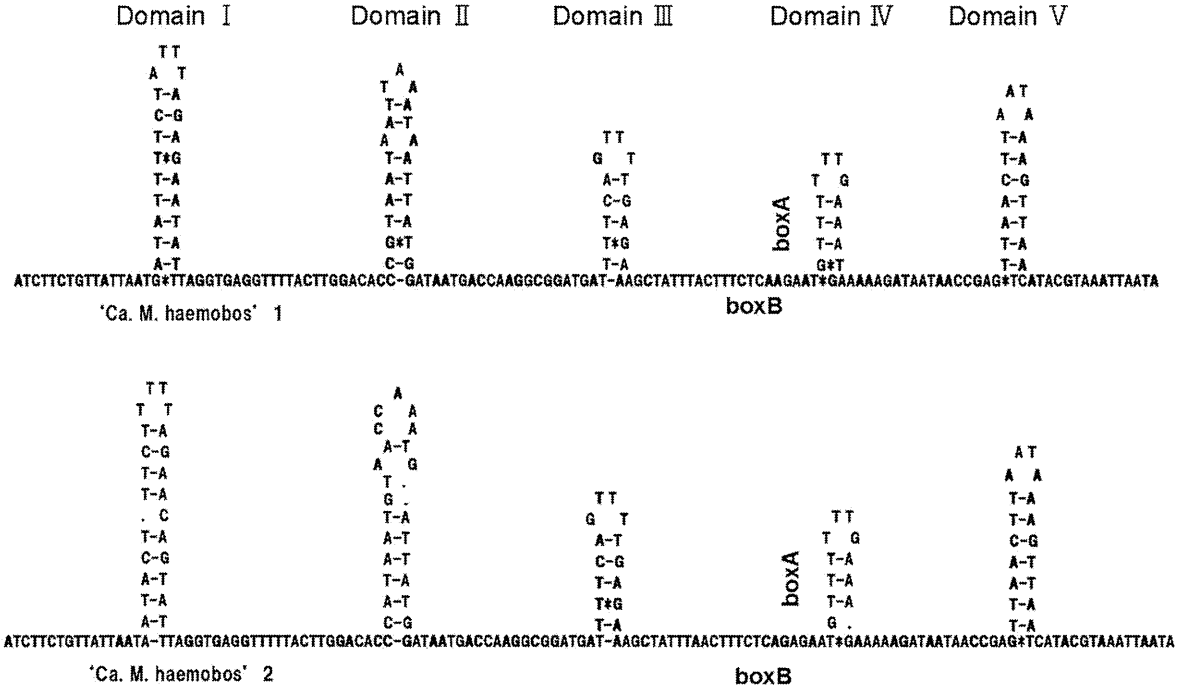

Fig. 2. Hypothetical secondary structures for the ITS regions of '*Ca.* M. haemobos' type 1 (top) and '*Ca.* M. haemobos' type 2 (bottom). Canonical Franklin-Watson-Crick base-pairing is hyphened, and a wobble base-pairing tolerated in the secondary structure is shown by an asterisk. The boxA was a part of the stem region of domain IV, and boxB was located between domains III and IV.

plasmas, lacking spacer tRNA genes and having boxA and boxB motifs [15].

In conclusion, 2 genotypes of '*Ca.* M. haemobos' were demonstrated by analyzing the primary and secondary structures of ITS regions. This may provide a clue to elucidate differences in severity of anemia in cattle, though virulence of these 2 genotypes remained unexplored. These genotypes can also be used for a genetic marker for bovine hemoplasma infections.

ACKNOWLEDGMENTS. This study was partly supported by a Grant-in-Aid (No. 23658251) for Scientific Research of the Japan Society for the Promotion of Science from the Ministry of Education, Culture, Sports, Science, and Technology of Japan.

REFERENCES

1. Harasawa, R. 1996. PCR: application of nested PCR to detection of mycoplasmas. pp.75–79. *In*: Molecular and Diagnostic Procedures in Mycoplasmology, vol. 2.(Razin, S. and Tully, J.G. eds.), Academic Press, New York.
2. Harasawa, R. 1999. Genetic relationships among mycoplasmas based on the 16S-23S rRNA spacer sequence. *Microbiol. Immunol.* **43**: 127–132. [Medline]
3. Harasawa, R., Hotzel, H. and Sachse, K. 2000. Comparison of the 16S-23S rRNA intergenic spacer regions among strains of the *Mycoplasma mycoides* cluster, and reassessment of the taxonomic position of *Mycoplasma* sp. bovine group 7. *Int. J. Syst. Evol. Microbiol.* **50**: 1325–1329. [Medline] [CrossRef]
4. Harasawa, R. and Kanamoto, Y. 1999. Differentiation of two biovars of *Ureaplasma urealyticum* based on the 16S-23S rRNA intergenic spacer region. *J. Clin. Microbiol.* **37**: 4135–4138. [Medline]
5. Harasawa, R., Kawahara, M. and Rikihisa, Y. 2002. Character-

istics of the 16S-23S rRNA intergenic spacer region of *Mycoplasma haemomuris*, previously classified as '*Haemobartonella muris*'. *J. Vet. Med. Sci.* **64**: 1161–1164. [Medline] [CrossRef]
6. Harasawa, R., Lefkowitz, E. J., Glass, J. I. and Cassell, G. H. 1996. Phylogenetic analysis of the 16S-23S rRNA intergenic spacer region of the genus *Ureaplasma*. *J. Vet. Med. Sci.* **58**: 191–195. [Medline] [CrossRef]
7. Harasawa, R., Mizusawa, H., Fuji, M., Yamamoto, J., Mukai, H., Uemori, T., Asada, K. and Kato, I. 2005. Rapid detection and differentiation of the major mycoplasma contaminants in cell cultures using real-time PCR with SYBR Green I and melting curve analysis. *Microbiol. Immunol.* **49**: 859–863. [Medline]
8. Harasawa, R., Pitcher, D. G., Ramirez, A. S. and Bradbury, J. M. 2004. A putative transposase gene in the 16S-23S rRNA intergenic spacer region of *Mycoplasma imitans*. *Microbiology* **150**: 1023–1029. [Medline] [CrossRef]
9. Harasawa, R., Uemori, T., Asada, K., Kato, I. and Shiragami, N. 1992. 'boxA'-like sequence between the 16S/23S spacer in the rRNA operon. *FEBS Lett.* **297**: 209–211. [Medline] [CrossRef]
10. Hoelzle, K., Hofmann-Lehmann, R. and Hoelzle, L. E. 2010. '*Candidatus* Mycoplasma haemobos', a new bovine haemotrophic Mycoplasma species? *Vet. Microbiol.* **144**: 525–526. [Medline] [CrossRef]
11. Hoelzle, K., Winkler, M., Kramer, M. M., Wittenbrink, M. M., Dieckmann, S. M. and Hoelze, L. E. 2011. Detection of *Candidatus* Mycoplasma haemobos in cattle with anemia. *Vet. J.* **187**: 408–410. [Medline] [CrossRef]
12. Hofmann-Lehmann, R., Meli, M. L., Dreher, U. M., Gönczi, E., Deplazes, P., Braun, U., Engels, M., Schüpbach, J., Jörger, K., Thoma, R., Griot, C., Stark, K. D. C., Willi, B., Schmidt, J., Kocan, K. M. and Lutz, H. 2004. Concurrent infections with vector-borne pathogens associated with fetal hemolytic anemia in a cattle herd in Switerland. *J. Clin. Microbiol.* **42**: 3775–3780. [Medline] [CrossRef]
13. Nishizawa, I., Sato, M., Fujihara, M., Sato, S. and Harasawa, R. 2010. Differential detection of hemotropic *Mycoplasma* species in cattle by melting curve analysis of PCR products. *J. Vet. Med. Sci.* **72**: 77–79. (Erratum. *J. Vet. Med. Sci.* 72: 1704.) [Medline] [CrossRef]
14. Saitou, N. and Nei, M. 1987. The neighbor-joining method: a new method for reconstructing phylogenetic trees. *Mol. Biol. Evol.* **4**: 406–425. [Medline]
15. Sasaoka, F., Suzuki, J., Fujihara, M., Watanabe, Y., Nagai, K. and Harasawa, R. 2012. Examination of the 16S-23S rRNA intergenic spacer sequences of '*Cadidatus* Mycoplasma haemobos' and *Mycoplasma haemofelis*. *J. Vet. Med. Sci.* 74: 83–87. [Medline] [CrossRef]
16. Su, Q. L., Song, H. Q., Lin, R. Q., Yuan, Z. G., Yang, J. F., Zhao, W. Y. and Zhu, X. Q. 2010. The detection of '*Candidatus* Mycoplasma haemobos' in cattle and buffalo in China. *Trop. Anim. Health Prod.* **42**: 1805–1808. [Medline] [CrossRef]
17. Tagawa, M., Matsumoto, K. and Inokuma, H. 2008. Molecular detection of *Mycoplasma wenyonii* and '*Candidatus* Mycoplasma haemobos' in cattle in Hokkaido, Japan. *Vet. Microbiol.* **132**: 177–180. [Medline] [CrossRef]
18. Tagawa, M., Matsumoto, K., Yokoyama, N. and Inokuma, H. 2010. Comparison of the effect of two hemoplasma species on hematological parameters in cattle. *J. Vet. Med. Sci.* **72**: 113–115. [Medline] [CrossRef]
19. Thompson, J. D., Higgins, D. G. and Gibson, T. J. 1994. CLUSTAL W: improving the sensitivity of progressive multiple sequence alignment through sequence weighting, position-specific gap penalties and weight matrix choice. *Nucleic Acids Res.* **22**: 4673–4680. [Medline] [CrossRef]
20. Uilenberg, G. 2009. '*Candidatus* Mycoplasma haemobos'. *Vet. Microbiol.* **138**: 200–201. [Medline] [CrossRef]
21. Zuker, M. and Stiegler, P. 1981. Optimal computer folding of large RNA sequences using thermodynamics and auxiliary. *Nucleic Acids Res.* **9**: 133–148. [Medline] [CrossRef]

academicJournals

Vol. 7(18), pp. 1780-1786, 30 April, 2013
DOI: 10.5897/AJMR12.1102
ISSN 1996-0808 ©2013 Academic Journals
http://www.academicjournals.org/AJMR

African Journal of Microbiology Research

Full Length Research Paper

Effects of urea on length distribution and morphology of *Escherichia coli* and *Salmonella enterica* subsp. *enterica* cells

Masatoshi FUJIHARA[1,2], Jun-ichi WAKITA[3], Daisuke KONDOH[2,4], Mitsugu MATSUSHITA[3] and Ryô HARASAWA[1, 2*]

[1]Laboratory of Veterinary Microbiology, Iwate University, 3-18-8 Ueda, Morioka, Iwate 020-8550, Japan.
[2]The United Graduate School of Veterinary Science, Gifu University, 1-1 Yanagido, Gifu, Gifu 501-1193, Japan.
[3]Department of Physics, Chuo University, 1-13-27 Kasuga, Bunkyo-ku, Tokyo 112-8551, Japan.
[4]Laboratory of Veterinary Anatomy, Iwate University, 3-18-8 Ueda, Morioka, Iwate 020-8550, Japan.

Accepted 19 April, 2013

Our previous studies showed that urea in acidic broth induced swarmer morphotypes in *Proteus mirabilis,* but the effects to other bacterial species remain unsolved. Here we report effects of urea on morphology and size distribution of urease-negative *Escherichia coli* and *Salmonella enterica* serovar Abony grown in urea-containing broth. Statistical analysis indicated lognormal distribution of the cellular lengths below a threshold level, suggesting that the growth process of bacterial cells obeys some random multiplicative process below a threshold value, despite any other factors affecting the process above the threshold value, to produce elongated cells. In urea broth, the distribution shifted to larger size and enormously elongated cells appeared. Morphological studies in urea broth revealed that filamentous cells of *E. coli* and *S.* Abony, accompanied with incomplete chromosomal segregation without forming hyperflagellates were induced at logarithmic growth phase, unlike swarmer cells in *P. mirabilis*. Since cell division protein FtsZ (filamenting temperature-sensitive mutant Z) assembled round the chromosome segregated point and cells were divided into short rods after cell counts had reached to a threshold level, urea in broth was responsible for delay of chromosomal segregation.

Key words: Chromosomal segregation, enterobacteria, filamentous cells, urea.

INTRODUCTION

Bacterial shapes differ among various genera, and it is a characteristic feature of some bacteria to grow and multiply in filaments, clusters or chains. All these morphological properties are of value in the identification and classification of bacterial strains, though a particular species may show variations of shape and size according to environments including nutrient conditions. For example, bacterial cells grown in rich nutrient medium are

*Corresponding author. Tel/Fax: +81-19-621-6158. E-mail: harasawatky@umin.ac.jp.

Abbreviations: BSA, Bovine serum albumin; **DAPI,** 4',6-diamidino-2-phenylindole; **EDTA,** ethylenediaminetetraacetic acid; **FtsZ,** filamenting temperature-sensitive mutant Z; **P2,** testing broth containing 2 g/L peptone; **P2U,** testing broth containing 2 g/L peptone and 25 g/L urea; **P50,** testing broth containing 50 g/L peptone; **P50U,** testing broth containing 50 g/L peptone and 25 g/L urea; **PBS,** phosphate buffered saline.

significantly larger than in nutrient-poor medium (Schaechter et al., 1958). The small cell sizes due to starvation conditions increase resistance to acid, oxidative stress and proteases (Clements and Foster, 1999; Watson et al., 1998). Although, other environmental factors such as temperature (Wiebe et al., 1992) and osmotic shock (Baldwin et al., 1988) have been reported to affect the size of bacteria, cell size reduction appears to be induced predominantly by nutrient limitation. On the other hand, harmful environments such as low water activity (Mattick et al., 2000), refrigerated temperature (Mattick et al., 2003), host innate immunity (Justice et al., 2006), high hydrostatic pressure (Ishii et al., 2004) and presence of chelating agents (Fujihara et al., 2009) inhibit bacterial cell division resulting in the production of filamentous cells by unknown mechanisms. Similarly, several antibacterial reagents blocking FtsZ, the tubulin homologue that forms cytokinetic Z ring (Löwe and Amos, 1998) are also known to yield filamentous cells (Beuria et al., 2005; Jaiswal et al., 2007; Wang et al., 2003).

We have previously demonstrated that urea, a denaturation agent for protein structure, induced swarmer morphotypes of *Proteus mirabilis* strains in acidic broth (Fujihara et al., 2011). Although, biological functions of urea remain largely undocumented, urea is known to delay cell cycles and induce apoptosis in eukaryotic cellls without inhibition of DNA synthesis (Michea et al., 2000). To assess the biological function of urea to enterobacteria, in the present study, we examined effects of urea to morphology and cell length distribution of urease-negative *Escherichia coli* and *Salmonella enterica* subsp. *enterica* serovar Abony.

MATERIALS AND METHODS

Bacterial strains and growth condition

Escherichia coli FDA strain (same progenitor of ATCC 25922) and *Salmonella enterica* subsp. *enterica* serovar Abony K103 strain (same progenitor of NCTC 6017) were grown in Luria broth (SIGMA-ALDRICH, Tokyo, Japan) for 18 h at 37°C. Testing broth consisting of 5 g sodium chloride, 5 g dipotassium hydrogen-phosphate, 0.651 g magnesium chloride hexahydrate and 2 or 50 g of Bacto-Peptone (Becton, Dickison and Company, Sparks, MD, U.S.A.) was supplemented with 25 g urea (P2U or P50U) or without urea (P2 or P50) in 1 L of distilled water. The amount of urea used in this study was based on the level of human urine (Griffith et al., 1976). The broth medium was adjusted to pH 7.1 and filter-sterilized.

Small amount of bacterial cells approximately 10^2 colony forming unit obtained from the Luria broth cultures were inoculated into the testing broth and incubated at 37°C. After 6, 8, 10, 12, 14 h incubation, living cells were counted by plating on MacConkey agar plates (NIHON Pharmaceutical, Tokyo, Japan).

Measuring of bacterial cell length

Bacterial cells were harvested after 8, 10 and 12 h incubation, since countable cells were not apparent until 6 h incubation. They were collected by centrifugation at 1,000 g for 1 and suspended in broth to adjust to an appropriate numbers of bacterial cells for observation using an Eclipse TE2000-U fluorescence microscope (Nikon, Tokyo, Japan) equipped with a VB-7010 digital camera (KEYENCE, Osaka, Japan). After the microscopic images recorded as color scale data were converted into binary data, the area of each bacterial cell was measured by numerical analysis software, MATLAB (MathWorks, Natick, MA, U.S.A.). Then, we calculated the length and the width of more than 1,000 bacterial cells from an area as described previously (Wakita et al., 2010).

Immunofluorescence microscopy

Chromosome and FtsZ ring organization were observed as described by Den Blaauwen et al. (1999) with a modification. Cells grown for 8 h were fixed in 2.8% neutral-buffered formalin and 0.04% glutaraldehyde for 15 min at ambient temperature. Cells were washed twice in phosphate buffered saline (PBS), pH 7.2, and subsequently suspended in 0.1% Triton X-100 in PBS for 45 min at ambient temperature. The cells were washed three times in PBS and resuspended in PBS containing 100 μg of lysozyme per ml and 5 mM ethylenediaminetetraacetic acid (EDTA) for 45 min at ambient temperature and then the cells were washed three times in PBS. FtsZ was stained with a polyclonal anti-FtsZ rabbit antibody (1:200; Agrisera, Vännas, Sweden) diluted in PBS containing 1% bovine serum albumin (BSA) for 2 h at 37°C. The cells were washed three times with PBS containing 0.05% (v/v) polyoxyeethlene sorbitan monolaurate. The cells were then treated with secondary antibodies, Cy3-conjugated goat anti-rabbit antibody (1:1000; Rockland Immunochemicals, Inc., Gilbertsville, PA, U.S.A.) diluted in PBS containing 1% BSA for 2 h at 37°C. The cells were further washed three times in PBS–0.05% polyoxyethylene sorbitan monolaurate.

In contrast, nucleoids were stained using 2.5 μg/ml of 4',6-diamidino-2-phenylindole (DAPI) (Dojindo, Kumamoto, Japan) and visualized with a fluorescence microscope Eclipse TE2000-U. Images were captured and submerged by using a VB-7010 digital camera.

RESULTS

Growth curve

Growth curve of both bacterial strains were shown in Figure 1. Although, no marked difference in growth speed was evident depending on the concentration of peptone, viable bacterial counts in the stationary phase increased under the conditions of high level of peptone. On the other hand, addition of urea delayed the proliferation. Higher cell counts were measured in P2 and P50 as compared to P2U and P50U after 8 h incubation, though after 12 h incubation higher counts were obtained in broth of higher concentration of peptone irrespective of addition of urea.

Statistical analysis of bacterial cell length distribution

Cell length distributions after 8, 10 and 12 h were shown in Table 1. Average cell length was longer in the logarithmic growth phase in all the broth media. In

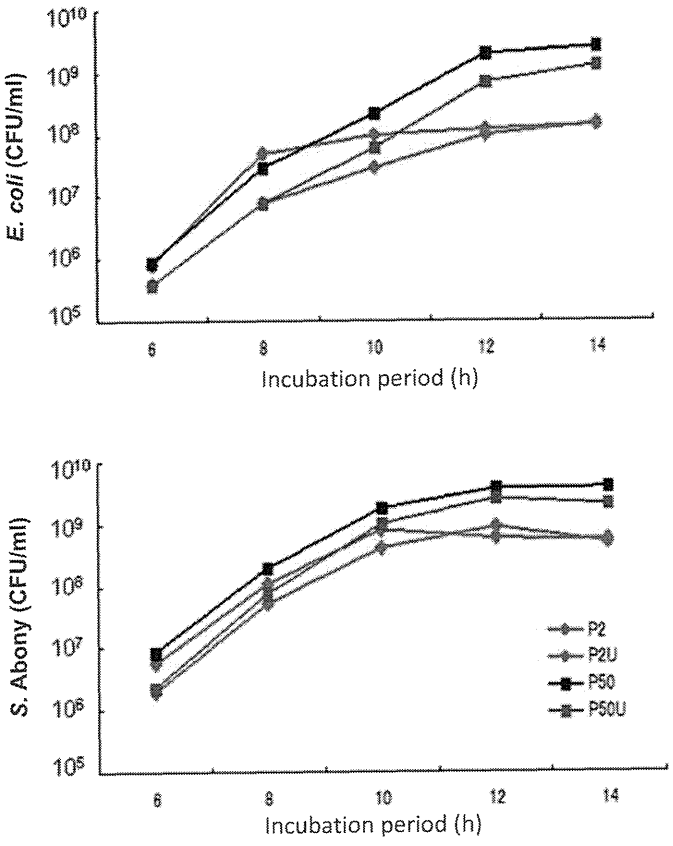

Figure 1. Growth curves of *E. coli* and *S.* Abony in broth. About 100 bacterial cells were inoculated in each broth and after 6, 8, 10, 12, 14 h incubation at 37°C; living bacterial cells were counted by plating on MacConkey agar plates.

addition, cells increased length in P50 rather than in P2. In urea-containing broth, the highest counts of cells over 5 m long were seen in the logarithmic phase and cells had divided into shorter rods along with growth. The microscopic observation revealed that elongated cells divided irregularly into short and long cells. Similarly with average of cell length, P50U produced highest counts of *E. coli* cells longer than 10 m, whereas P2U did in *S.* Abony. The probability densities of cell length about *E. coli* and *S.* Abony after 8 h incubation are shown in Figure 2a and b, respectively. It is noticed that the distributions with urea shift to longer direction of cell length from that without urea. Furthermore, all the distributions in Figure 2a and b have thick tails. It just reminds us of lognormal distribution.

Figure 2c and d show that the cumulative length distributions are well fitted except the tail part by the solid curves which are lognormal distributions in cumulative form given by:

$$N(x)=\frac{1}{2}\left(1-\mathrm{erf}\left[\frac{\ln(x/L)}{\sqrt{2}\sigma}\right]\right)$$

Where x, σ and L are the length, the standard deviation, and the median, respectively. $\mathrm{erf}(z)$ is the error function defined by

$$\mathrm{erf}(z)=\left(2/\sqrt{\pi}\right)\int_0^z \exp(-y^2)\mathrm{d}y$$

After 10 and 12 h incubation, cell length distribution had shifted to shorter direction (data not shown).

Effects of urea on the chromosome and cytokinetic Z ring organization

We examined the effects of urea on Z ring assembly and karyomitosis by fluoresence microscopy (Figure 3). While the chromosome of short rods grown in urea-negative broth replicated by binary fission and Z rings located at the middle of cells, the multiple chromosomes distributed haphazardly in elongated cells grown in broth containing urea. The lateral length of nucleoid in elongated cells was not equal and chromosomal segregation was not seen in the middle of cells. FtsZ assembled round the point of karyomitosis as well as cells grown in broth without urea. No bacterial cells were stained in negative controls without anti-FtsZ antibody.

DISCUSSION

In the present study, broth medium containing urea induced elongated cells during logarithmic phase of growth, though optimum peptone concentration was different between *E. coli* and *S.* Abony. Most elongated cells had divided into short rods after stationary phase. In general, cell length and DNA content start to decrease transition point between the logarithmic phase and the stationary phase (Akerlund et al., 1995) and cells grown in nutrient-rich medium exhibit longer cell length than in nutrient-poor medium (Schachter et al., 1958). Our findings in broth medium without urea confirmed this, but P2U shifted to longer length in large majority of *S.* Abony cells than P50U. It remained unclear why optimal peptone concentration to produce elongated cells was different between *E. coli* and *S.* Abony. Polymerization of FtsZ, one of the central cell division proteins (Madabhushi and Marians, 2009) depends on multiple factors including pH, concentrations of magnesium, potassium, calcium, competing nucleotide tri-phosphates, macromolecular crowding and the presence of FtsZ interacting proteins (González et al., 2003; Mukherjee and Lutkenhaus, 1998, 1999; Mukherjee et al., 1998).

Inhibitors such as antibiotics against Fts proteins were known to produce filamentous cells, though they did not affect karyomitosis (Beuria et al., 2005; Jaiswal et al., 2007). Additionally, induction of *sulA* (*sfiA*), one of the SOS genes, also mediates inhibition of FtsZ assembly without influence on karyomitosis in *E. coli* (Bernhardt

Table 1. Cell length distributions after 8, 10, 12 h incubation. More than 1,000 cell lengths were measured and the abundance ratio of shorter than 5, 5 to 10, 10 to 20, 20 to 30, 30 to 40, 40 to 50 μm and longer than 50 μm was shown.

	Broth	Incubation period (h)	Measured cell number	Average±S.D. (μm)	Cell length (μm) distribution (%)							Max (μm)
					>5	5-10	10-20	20-30	30-40	40-50	50<	
E. coli	P2	8	1999	3.211±0.011	93.7	6.2	0.1	0	0	0	0	12.1
		10	1379	2.912±0.010	97.6	2.4	0	0	0	0	0	6.8
		12	1189	2.467±0.009	99.1	0.8	0.1	0	0	0	0	10.1
	P2U	8	1095	5.538±0.014	40.2	53.1	5.1	1.0	0.2	0.3	0	44.5
		10	1383	4.049±0.014	74.5	23.7	1.6	0.1	0.1	0	0	36.1
		12	1302	2.967±0.012	93.3	6.1	0.4	0	0.2	0	0	31.6
	P50	8	1067	4.131±0.010	73.6	23.4	2.9	0.1	0	0	0	20.7
		10	1148	3.691±0.010	88.9	11.1	0.1	0	0	0	0	17.4
		12	4168	2.844±0.010	97.9	2.1	0	0	0	0	0	11.7
	P50U	8	1057	6.885±0.017	22.8	55.2	13.3	4.6	2.3	1.1	0.7	112.5
		10	1469	6.610±0.016	25.5	54.9	13.5	3.8	0.8	0.7	0.7	152.3
		12	2675	5.319±0.014	45.1	48.1	4.7	1.5	0.7	0.1	0.3	97.4
S. Abony	P2	8	2485	2.879±0.011	97.5	2.5	0.1	0	0	0	0	16.0
		10	2026	2.595±0.011	99.1	0.9	0	0	0	0	0	10.5
		12	1748	2.288±0.010	99.3	0.7	0	0	0	0	0	8.4
	P2U	8	1350	5.785±0.016	37.2	52.7	8.6	1.1	0.2	0	0.1	93.9
		10	2838	3.653±0.016	79.0	18.0	2.2	0.6	0.2	0	0	58.6
		12	1709	3.119±0.015	89.1	8.8	1.8	0.2	0	0	0	31.25
	P50	8	1117	3.754±0.011	85.1	14.9	0	0	0	0	0	9.9
		10	1270	2.912±0.009	88.9	11.0	0.1	0	0	0	0	23.4
		12	1057	2.375±0.008	99.8	0.2	0	0	0	0	0	6.6
	P50U	8	1045	4.322±0.019	70.9	28.6	0.5	0	0	0	0	14.2
		10	1118	3.989±0.013	76.7	22.5	0.8	0	0	0	0	16.9
		12	1168	3.015±0.010	95.7	4.2	0.1	0	0	0	0	15.8

and de Boer, 2005; Mukherjee et al., 1998). Urea in broth did not inhibit assembly of FtsZ despite random segregation of chromosomes, though formation of matured Z ring was not explored in the present study. Therefore, it is most likely that appearance of filamentous cells was due to delay

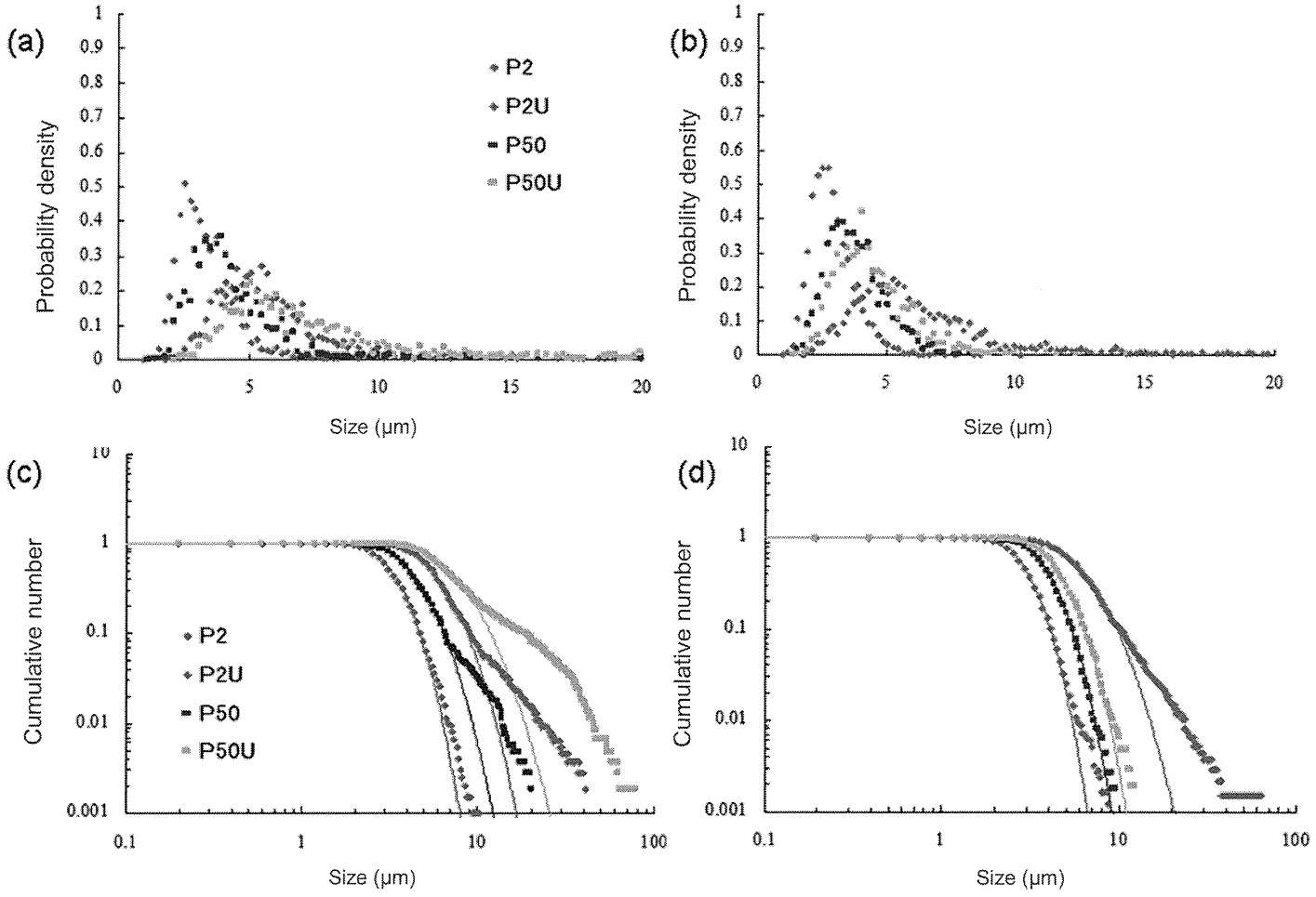

Figure 2. Probability density (a: *E. coli,* b: *S.* Abony) and cumulative distributions (c: *E. coli*, d: *S.* Abony) of bacterial cell length. The distributions of *E. coli* and *S.* Abony after 8 h incubation are shown and fitted by solid curves which are the lognormal distributions in cumulative form. Total numbers of bacterial cells are normalized to one.

of chromosomal segregation. Since normal segregation of chromosomes was evident in swarmer cells in *P. mirabilis* (Fujihara et al., 2011), appearance of filamentous cells in urea-containing broth may be accounted by another mechanism distinct from differentiation of swarmer cells. In addition, statistic distribution of bacterial cell length showed a lognormal distribution under growing process that was consistent with those commonly observed in each body growth according to a random multiplicative stochastic process (Walita et al., 2010). Thus, our data demonstrated also quantity of the temporal cell length and the effects of urea on bacterial cell division, while to identify the statistical characteristics of bacterial growth process.

In conclusion, we demonstrated urea-containing broth medium induced elongated cells in logarithmic phase of growth of enterobacteria, though exact mechanism remained unsolved. FtsZ localized at the chromosome-segregated point, despite yielding short and long cells at rondom from the elongated cells. We indicated cumulative distribution of bacterial lengths for *E. coli* in P50 and P50U, and for *S.* Abony in P2 and P2U were lognormal after 8 h incubation except for the tail part of the distributions along with an evidence for a threshold value of cell lengths. This implies that the growth process of bacterial cells obeys some random multiplicative process below a threshold value, despite any other factors affecting the process above the threshold value, to produce elongated cells. In urea-containing broth, the distribution shifted to larger size and enormously elongated cells appeared.

ACKNOWLEDGEMENTS

The authors are grateful to Dr. K. Omoe of the Food Security Laboratory for the gift of bacterial strains. M. F. wishes to acknowledge the support from Japan Society for the Promotion of Science (JSPS) for Japanese Junior Scientists. This work was supported by Grant-in-Aid for JSPS Fellows 22-2507.

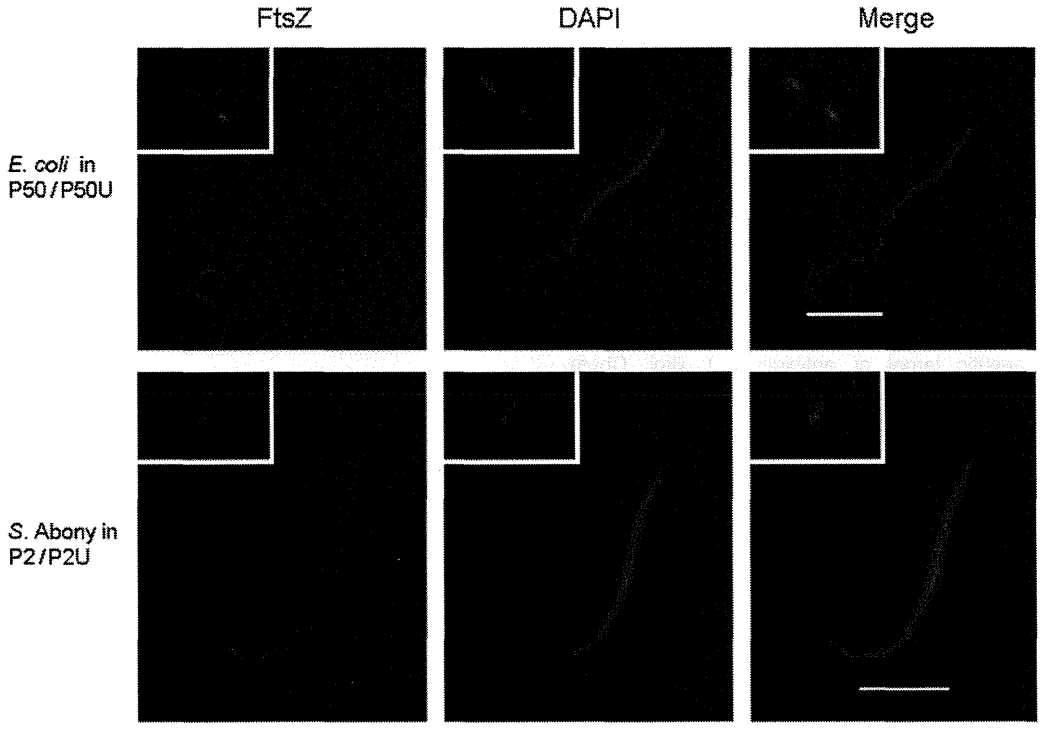

Figure 3. Fluorescence micrograph of *E. coli* grown in P50/P50U and *S.* Abony in P2/P2U grown for 8 h. Short cells in broth without urea are shown in upper left windows and these windows are same magnification as larger windows showing elongated cells in urea broth. Cells were immunostained with polyclonal anti-FtsZ rabbit antibody followed by Cy3-conjugated goat anti-rabbit secondary antibody. Nucleoids were visualized by treating the cells with DAPI. FtsZ is shown in red, and the DAPI-stained nucleoids are shown in blue. Bar = 10 μm.

REFERENCES

Akerlund T, Nordström K, Bernander R (1995). Analysis of cell size and DNA content in exponentially growing and stationary-phase batch cultures of *Escherichia coli*. J. Bacteriol. 177:6791-6797.

Baldwin WW, Sheu MJT, Bankston PW, Woldringh CL (1988). Changes in buoyant density and cell size of *Escherichia coli* in response to osmotic shocks. J. Bacteriol. 170:452-455.

Bernhardt TG, de Boer PA (2005). SlmA, a Nucleoid-associated, FtsZ binding protein required for blocking septal ring assembly over chromosomes in *E. coli*. Mol. Cell 18:555-564.

Beuria TK, Santra MK, Panda D (2005). Sanguinarine blocks cytokinesis in bacteria by inhibiting FtsZ assembly and bundling. Biochemistry 44:16584–16593.

Clements MO, Foster SJ (1999). Stress resistance in *Staphylococcus aureus*. Trends Microbiol. 7:458-462.

Den Blaauwen T, Buddelmeijer N, Aarsman ME, Hameete CM, Nanninga N (1999). Timing of FtsZ assembly in *Escherichia coli*. J. Bacteriol. 181:5167-5175.

Fujihara M, Maeda K, Sasamori E, Matsushita M, Harasawa R (2009). Effects of chelating reagents on colonial appearance of *Paenibacillus alvei* isolated from canine oral cavity. J. Vet. Med. Sci. 71:147-153.

Fujihara M, Obara H, Watanabe Y, Ono HK, Sasaki J, Goryo M, Harasawa R (2011). Acidic environments induce differentiation of *Proteus mirabilis* into swarmer morphotypes. Microbiol. Immunol. 55:489-493.

González JM, Jiménez M, Vélez M, Mingorance J, Andreu JM, Vicente M, Rivas G (2003). Essential cell division protein FtsZ assembles into one monomer-thick ribbons under conditions resembling the crowded intracellular environment. J. Biol. Chem. 278:37664-37671.

Griffith DP, Musher DM, Itin C (1976). Urease. The primary cause of infection-induced urinary stones. Investig. Urol. 13:346-350.

Ishii A, Sato T, Wachi M, Nagai K, Kato C (2004). Effects of high hydrostatic pressure on bacterial cytoskeleton FtsZ polymers in vivo and in vitro. Microbiology 150:1965-1972.

Jaiswal R, Beuria TK, Mohan R, Mahajan SK, Panda D (2007). Totarol inhibits bacterial cytokinesis by perturbing the assembly dynamics of FtsZ. Biochemistry 46:4211-4220.

Justice SS, Hunstad DA, Seed PC, Hultgren SJ (2006). Filamentation by *Escherichia coli* subverts innate defenses during urinary tract infection. Proc. Natl. Acad. Sci. USA. 103:19884-19889.

Löwe J, Amos LA (1998). Crystal structure of the bacterial cell-division protein FtsZ. Nature 391:203-206.

Madabhushi R, Marians KJ (2009). Actin homolog MreB affects chromosome segregation by regulating topoisomerase IV in *Escherichia coli*. Mol. Cell 33:171-180.

Mattick KL, Jørgensen F, Legan JD, Cole MB, Porter J, Lappin-Scott HM, Humphrey TJ (2000). Survival and filamentation of *Salmonella enterica* serovar Enteritidis PT4 and *Salmonella enterica* serovar Typhimurium DT104 at low water activity. Appl. Environ. Microbiol. 66:1274-1279.

Mattick KL, Phillips LE, Jørgensen F, Lappin-Scott HM, Humphrey TJ (2003). Filament formation by *Salmonella spp.* inoculated into liquid food matrices at refrigeration temperatures, and growth patterns when warmed. J. Food. Prot. 66:215-219.

Michea L, Ferguson DR, Peters EM, Andrews PM, Kirby MR, Burg MB (2000). Cell cycle delay and apoptosis are induced by high salt and urea in renal medullary cells. Am. J. Physiol. Renal Physiol. 278:209-218.

Mukherjee A, Cao C, Lutkenhaus J (1998). Inhibition of FtsZ polymerization by SulA, an inhibitor of septation in *Escherichia coli*. Proc. Natl. Acad. Sci. USA. 95:2885-2890.

Mukherjee A, Lutkenhaus J (1998). Dynamic assembly of FtsZ regulated by GTP hydrolysis. EMBO J. 17:462-469.

Mukherjee A, Lutkenhaus, J (1999). Analysis of FtsZ assembly by light scattering and determination of the role of divalent metal cations. J. Bacteriol. 181:823-832.

Schaechter M, Maaloe O, Kjeldgaard NO (1958). Dependency on medium and temperature of cell size and chemical composition during balanced grown of *Salmonella typhimurium*. J. Gen. Microbiol. 19:592-606.

Wakita J, Kuninaka H, Matsuyama T, Matsushita M (2010). Size distribution of bacterial cells in homogeneously spreading disk-like colonies by *Bacillus subtilis.* J. Phys. Soc. Jpn. 79:094002, DOI: 10.1143/JPSJ.79.094002.

Wang J, Galgoci A, Kodali S, Herath KB, Jayasuriya H, Dorso K, Vicente F, Gonzalez A, Cully D, Bramhill D, Singh S (2003). Discovery of a small molecule that inhibits cell division by blocking FtsZ, a novel therapeutic target of antibiotics. J. Biol. Chem. 278:44424–44428.

Watson SP, Clements MO, Foster SJ (1998). Characterization of the starvation-survival response of *Staphylococcus aureus*. J. Bacteriol. 180:1750-1758.

Wiebe WJ, Sheldon Jr WM, Pomeroy LR (1992). Bacterial growth in the cold: Evidence for an enhanced substrate requirement. Appl. Environ. Microbiol. 58:359-364.

NOTE *Bacteriology*

Two Clusters among *Mycoplasma haemomuris* Strains, Defined by the 16S-23S rRNA Intergenic Transcribed Spacer Sequences

Hinako SASHIDA[1)], Fumina SASAOKA[1)], Jin SUZUKI[1)], Masatoshi FUJIHARA[1)], Kazuya NAGAI[2)], Hiromi FUJITA[3)], Teruki KADOSAKA[4)], Shuji ANDO[5)] and Ryô HARASAWA[1)]*

[1)]*Department of Veterinary Microbiology, Faculty of Agriculture, Iwate University, Morioka 020–8550, Japan*
[2)]*Cryobiofrontier Research Center, Faculty of Agriculture, Iwate University, Morioka 020–8550, Japan*
[3)]*Mahara Institute of Medical Acarology, Anan 779–1510, Japan*
[4)]*Department of Infection and Immunology, Aichi Medical University, Nagakute 480–1195, Japan*
[5)]*Department of Virology 1, National Institute of Infectious Diseases, Tokyo 162–8640, Japan*

(Received 28 October 2012/Accepted 28 November 2012/Published online in J-STAGE 12 December 2012)

ABSTRACT. *Mycoplasma haemomuris* is a causative organism of infectious anemia or splenomegaly in rodents. Here we report two distinct genetic groups among *M. haemomuris* strains detected from rats and mice, respectively, by examining the nucleotide sequences of the 16S-23S rRNA intergenic transcribed spacer region that has been shown to be a stable genetic marker for mycoplasma species. Our results may reveal host-tropism of each cluster of *M. haemomuris* strains, and suggest an idea to distinguish *M. haemomuris* into two different genetic clusters.
KEY WORDS: hemoplasma, mycoplasma, rRNA

doi: 10.1292/jvms.12-0472; *J. Vet. Med. Sci.* 75(5): 643–648, 2013

Hemotropic mycoplasmas also called hemoplasmas are causative of infectious anemia in various mammalian animals [15]. Hemoplasma strains have been isolated as an anemic pathogen from rodents including mice, rats and hamsters and had once been identified by only microscopic observation of blood smears [18]. Hemoplasma infections in laboratory rodents have been concerned to undermine the validity of animal experiments [1, 13]. They are often unrecognized, because of clinically silent infections. Such latent infections have been reported in Sprague-Dawley and Wistar rats [2, 3]. Currently, only one hemoplasma species *Mycoplasma haemomuris* Mayer 1921 formerly *Bartonella muris* or *Haemobartonella muris*, is established in rodents [16, 17]. Nucleotide sequence of the 16S rRNA gene of *M. haemomuris* has been determined on the Shizuoka strain that was the only strain maintained *in vivo* at that time [19]. Subsequently, nucleotide sequence of the 16S-23S rRNA intergenic transcribed spacer (ITS) region of the same strain was defined [10]. However, genetic variation in the 16S rRNA gene or ITS region remains unexplored, because no other rodent hemoplasma strains except for the Shizuoka strain have been available. Here we report two genetic clusters in *M. haemomuris* strains by examining nucleotide sequence of ITS region as well as the 16S rRNA gene.

Anti-coagulated blood or spleen homogenates were obtained from black rats (*Rattus rattus*) or small field mice (*Apodemus argenteus*) infected with hemotropic mycoplasmas in Aomori and Fukushima Prefectures [5], and from black rats with splenomegaly trapped in Okinawa Prefecture, Japan. Detail of these samples examined is given in Table 1. Blood smears were prepared for Giemsa staining. Total DNA was extracted from 200 μl of the whole blood or spleen homogenate by using the QIAamp DNA Blood Mini Kit (QIAGEN, Hilden, Germany) according to the manufacturer's instructions, eluting into 200 μl of buffer AE, and stored at −20°C until examination in the PCR assay.

Seven DNA samples were subjected to PCR to amplify entire region of the 16S rRNA gene and ITS region. The PCR was carried out with 50-μl reaction mixtures containing 1 μl of DNA solution, 0.8 μl of Tks Gflex ™ DNA polymerase (5 units/μl), 25 μl of 2X Gflex PCR Buffer, 0.2 μl of relevant forward and reverse primers and water to a final volume of 50 μl. The forward (5′-AGAGTTTGATCCTGGCTCAG-3′, equivalent to nucleotide numbers 11 to 30 of *M. wenyonii*(AY946266), or 5′- ATATTCCTACGGGAAGCAGC-3′, equivalent to nucleotide numbers 328 to 347 of *M. wenyonii*), and reverse (5′- ACCGCAGCTGCTGGCACATA-3′, equivalent to nucleotide numbers 503 to 522 of *M. wenyonii*, or 5′-TACCTTGTTACGACTTAACT-3′, equivalent to nucleotide numbers 1446 to 1465 of *M. wenyonii*) (50 pmol/μl each) primers were used to amplify the 16S rRNA gene. On the other hand, ITS region was amplified by using forward primer Hemo16-23S-F (5′-GTTCCCAGGTCTTGTACACA-3′) and reverse primer Hemo16-23S-R1 (5′-CAGTACTTGTTCACTGGTA-3′) as described previously [6]. After initial denaturation at 94°C for 5 min, the reaction cycle was carried out 30 times with denaturation at 98°C for 10 sec, annealing at 55°C for 60 sec and extension at 68°C for 30 sec in a thermal cycler. The PCR products were fractionated on horizontal, submerged 1.0% SeaKem ME agarose gels (FMC Bioproducts, Rockland, ME, U.S.A.) in TAE (40 mM Tris, pH8.0, 5 mM

*CORRESPONDENCE TO: HARASAWA, R., The Iwate Research Center for Wildlife Diseases, Morioka 020–0816, Japan.
e-mail: harasawa-tky@umin.ac.jp

Table 1. Source of the samples examined in the present study

Sample designation	Host animal	Place of animal trapped (Prefecture, City)	Date of sampling	Condition of sample
Ikemajima 5–1	Black rat	Okinawa, Ikemajima	1-Sep-10	Whole blood
Ikemajima 14–1	Black rat	Okinawa, Ikemajima	1-Sep-10	Whole blood
S151-2	Small field mouse	Fukushima, Fukushima	15-Dec-85	Erythrocyte suspension
S152-2–4	Small field mouse	Fukushima, Fukushima	22-Mar-86	Spleen homogenate
S152-5–7	Small field mouse	Fukushima, Fukushima	22-Mar-86	Spleen homogenate
S154	Black rat	Fukushima, Kawamata	22-Feb-87	Spleen homogenate
S159-11–13	Small field mouse	Aomori, Owani	29-May-88	Spleen homogenate

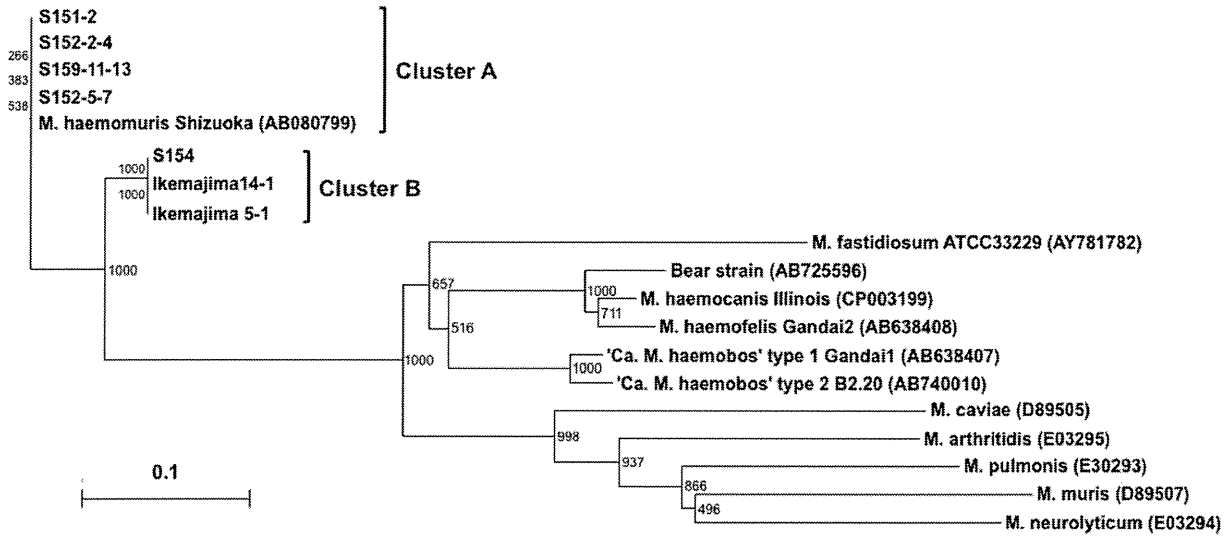

Fig. 1. Phylogenetic tree based on the hemoplasma ITS comparison with other rodent mycoplasmas. Following nucleotide sequence obtained from the DNA databases is shown with an accession number in parenthesis. They are *M. pulmonis* m53 (E03293), *M. neurolyticum* Sabin Type A (E03294), *M. arthritidis* PG6 (E03295), *M. caviae* G122 (D89505), *M. muris* RIII4 (D89507), *M. haemomuris* Shizuoka (AB080799), *M. haemofelis* Gandai2 (AB638408), Bear hemoplasma strain (AB725596), '*Ca.* M. haemobos' type1 Gandai1 (AB638407), and '*Ca.* M. haemobos' type 2 B2.20 (AB740010). *Mycoplasma fastidiosum* ATCC33229 (AY781782) was included as an out-group. Scale bar indicates the estimated evolutionary distance that was computed with CLUSTAL W [24] using neighbor-joining method [20]. Numbers in the relevant branches refer to the values of boot-strap probability of 1,000 replications.

sodium acetate and 1 mM disodium ethylenediaminetetraacetate) buffer at 50 volts for 60 min. After electrophoresis, the gels were stained in ethidium bromide solution (0.4 μg/m*l*) for 15 min and visualized under UV transilluminator. DNA in a clearly visible band was extracted by using NucleoSpin Extract II kit (Macherey-Nagel, Düren, Germany) and was subjected to direct sequencing in a 3500 Genetic Analyzer (Applied Biosystems, Foster City, CA, U.S.A.).

Almost entire nucleotide sequences of the 16S rRNA gene and ITS region of the seven strains were successfully determined. Nucleotide sequences of the 16S rRNA gene of these samples were almost identical (99% homology) and also showed 99% homology to those of *M. haemomuris* Shizuoka strain (accession number U82963) isolated from a small field mouse in Japan [19]. This allowed us to classify the seven strains as *M. haemomuris*, though the Shizuoka strain used as a reference has been lost and unavailable (Rikihisa, personal communication). Hemoplasma species has provisionally been classified or identified by only nucleotide sequence of the 16S rRNA gene because of uncultivable trait [16, 17].

The nucleotide sequences of ITS of the seven strains were compared with those of authentic rodent mycoplasma species in a phylogenetic tree that was generated with the neighbor-joining method [20] from a distance matrix corrected for nucleotide substitutions by the Kimura two-parameter model [14]. Phylogenetic analysis indicated that the seven isolates were divided into two clusters A and B (Fig. 1). Nucleotide sequence similarity between these two clusters was 84.9%. This variation can be used for a genetic marker of *M. haemomuris* strains.

Next, we examined primary and secondary structures of the ITS region of the isolates. Nucleotide sequences of ITS region from the seven isolates were compared with six other hemoplasma sequences in an alignment created by

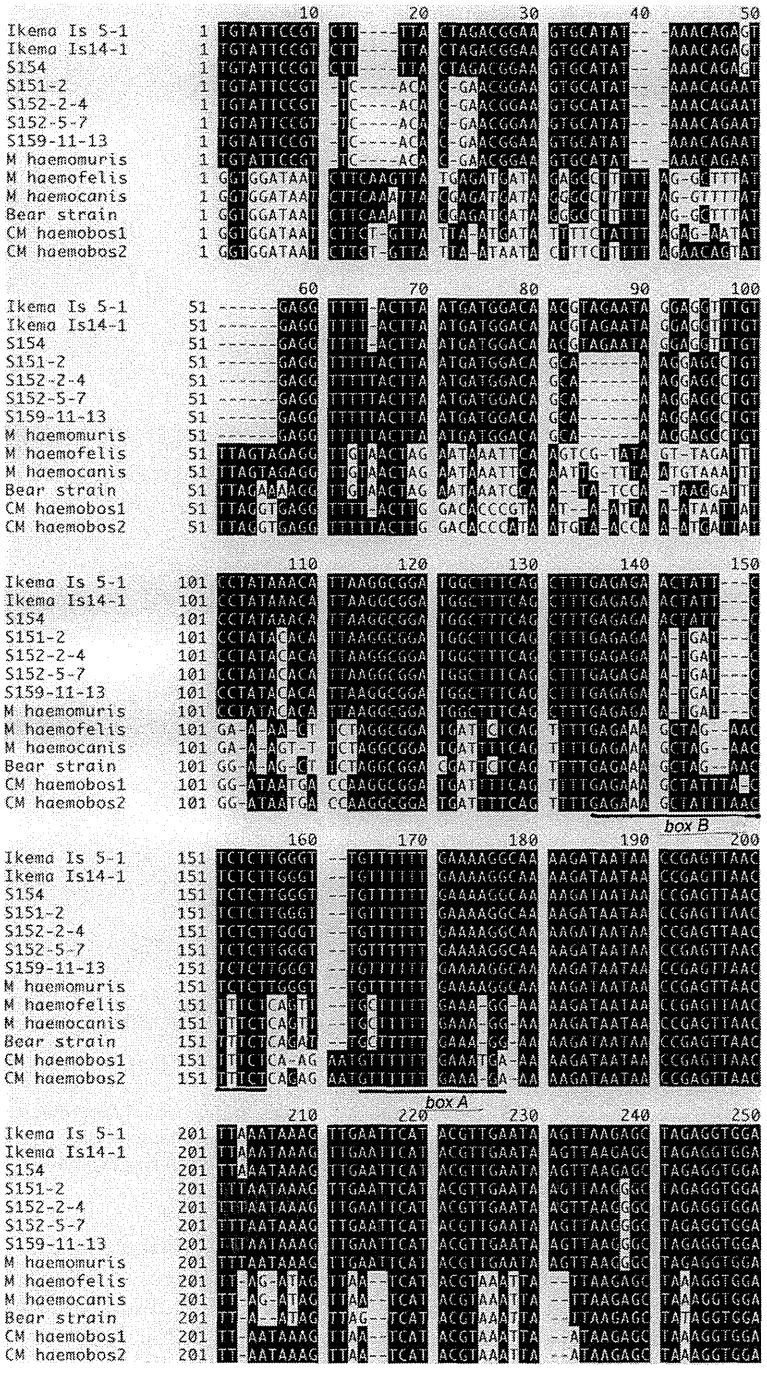

Fig. 2. Nucleotide variations appeared in alignment of the 13 ITS sequences from different hemoplasma strains. The nucleotide sequence numbers are given from a consensus sequence. Homologous nucleotides are shown as inverted characters. Dashes indicate nucleotide gaps between adjacent nucleotides introduced for the alignment. Ikema Is 5-1, Ikema Is14-1, CM haemobos1 and CM haemobos2 represent Ikemajima 5-1, Ikemajima 14-1 and '*Candidatus* M. haemobos' type 1 and type 2 [22] strains, respectively.

CLUSTAL W [24]. Of the seven strains, ITS sequences of the five strains consisting of S151-2, S152-2–4, S152-5–7 and S159-11–13 were distinct from three other strains, S154, Ikemajima 5–1 and Ikemajima 14–1 (Fig. 2). ITS sequences of these five strains were identical to those of *M. haemomuris* Shuzuoka strain. ITS region has been used for a comple-

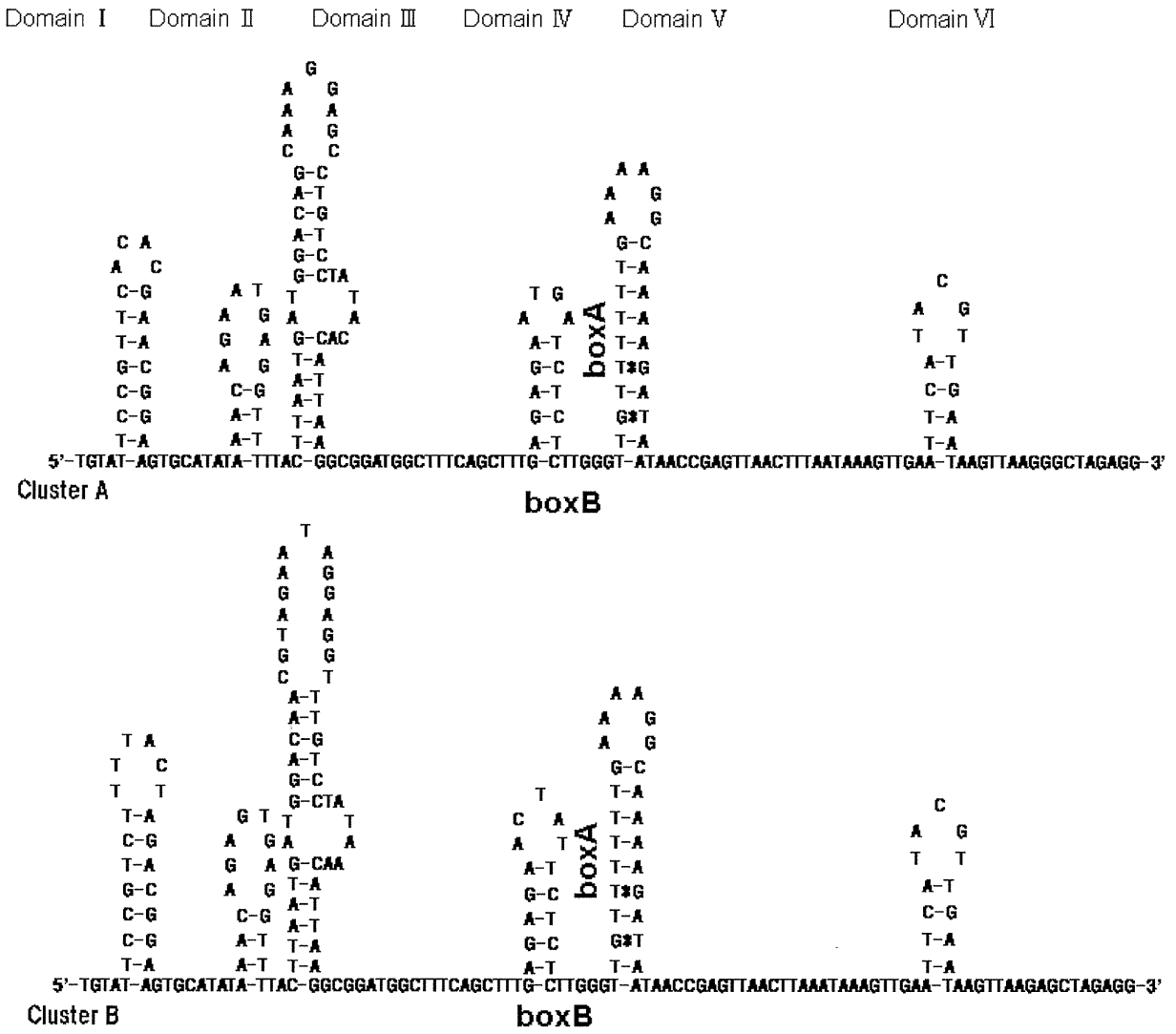

Fig. 3. Hypothetical secondary structures for the ITS regions of the two clusters, A (top) and B (bottom), of *M. haemomuris*. Canonical Franklin-Watson-Crick base-pairing is hyphened, and a wobble base-pairing tolerated in the secondary structure is shown by an asterisk. The box A was a part of the stem region of domain V, and box B was located between domains IV and V.

mentary genetic marker for identification and classification of mycoplasmas, since this region is characteristic to each *Mycoplasma* species [7–9, 11, 21, 25]. Thus, difference in nucleotide sequence of ITS region may raise a hypothesis that *M. haemomuris* species contains at least two distinct clusters. We also found the ITS region of seven strains lacked spacer tRNA gene, but contained box A and box B motifs previously identified in other mycoplasma species [12]. These motifs are obvious in the sequence alignment of ITS regions of these hemoplasmas.

The secondary structures of the ITS were predicted according to the algorithm of Zuker and Stiegler [26]. Six stem-loop domains were allocated in ITS region of the clusters A and B (Fig. 3). Domains V and VI were common between the clusters. Domain II was well conservative, despite a single nucleotide substitution at loop region. Stem region of domain IV was well conserved between the clusters. Secondary structures in ITS region have sometime provided a key character to distinguish closely related species of mycoplasmas [8, 9, 22]. Thus, in addition to our previous illustration of ITS for *M. haemomuris* [10], the present analysis revealed existence of two genetically distinct clusters among *M. haemomuris* strains.

Collective analyses on the primary and secondary structures of ITS indicated *M. haemomuris* strains were divided into two clusters. This variation may not attribute to a geographical difference of locations where the hemoplasmas isolated, because cluster A included strains from Fukushima, Aomori and Shizuoka Prefectures, and cluster B included Fukushima and Okinawa Prefectures. Thus, this variation is most likely to depend on difference of natural host of hemoplasmas. In fact, cluster A strains have been isolated

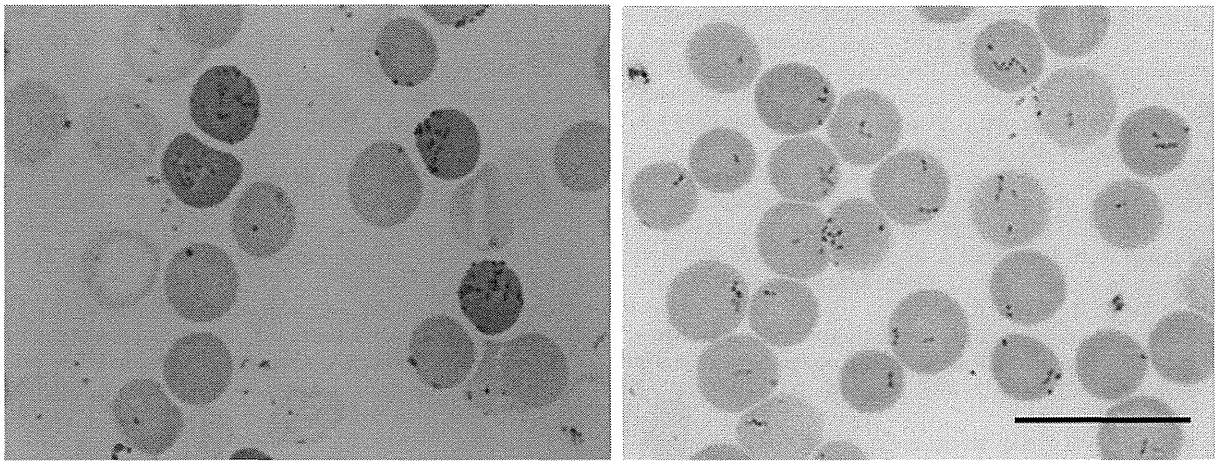

Fig. 4. Hemoplasma strains Ikemajima 5-1 (right) and S151-2 (left) from a black rat and a small field mouse, respectively, stained a deep purple color on blood smears. Bar represents 10 μm.

from small field mice, while cluster B was from black rats. *Mycoplasma haemomuris*, that was first observed in the blood of rats and named *Bartonella muris ratti* by Martin Mayer in 1921, was confirmed to be the causative agent of infectious anemia in albino rats following splenectomy [4]. Subsequently, another type of *Bartonella* morphologically distinct from *B. muris ratti* was found in the blood of albino mice by Schilling, and he called this variant as *B. muris musculi* [23]. Taken together, it turns out that the scientific designation, *M. haemomuris*, is composite of *B. muris* subsp. *ratti* in rat and *B. muris* subsp. *musculi* in mouse, despite possible cross-transfer between these animal species by experimental infection. Therefore, this raises a hypothesis that *M. haemomuris* Shizuoka strain isolated from a mouse may correspond to formerly *B. muris musculi*. In our microscopic observation, hemoplasma strains from each cluster appeared as tiny round bodies sometimes in chain within the red blood cells, though some of those from small filed mice might appear as projections from the red blood cell surface (Fig. 4). However, this minor difference may not be sufficient for differentiation of these two clusters on blood smears.

In conclusion, two genetic clusters of *M. haemomuris* were demonstrated by analyzing the primary and secondary structures of ITS region of *M. haemomuris* strains. Besides, our findings support the hypothesis that the cluster including *M. haemomuris* Shizuoka strain represents *M. haemomuris* subsp. *musculi*, and the another cluster corresponds to *M. haemomuris* subsp *ratti*. This may provide a clue to elucidate differences in severity of anemia in rodent, since virulence of these two clusters is currently unknown. This variation can also be used for a genetic marker for monitoring of *M. haemomuris* infections in laboratory rodents. The GenBank/EMBL/DDBJ accession numbers appeared for the first time in this study are AB758434 through AB758440.

ACKNOWLEDGMENT. This study was partly supported by a Grant-in-Aid (No. 23658251) for Scientific Research of the Japan Society for the Promotion of Science from the Ministry of Education, Culture, Sports, Science, and Technology of Japan.

REFERENCES

1. Baker, H. J., Cassell, G. H. and Lindsy, J. R. 1971. Research complications due to *Haemobartonella* and *Eperythrozoon* infections in experimental animals. *Am. J. Pathol.* **64**: 625–652. [Medline]
2. Bartlett, R. and Pease, P. 1975. Latent *Haemobartonella muris* infections: its transmission and decline in an inbred, ectoparasite-free strains of Wistar rat. *Parasitology* **71**: 35–40. [Medline] [CrossRef]
3. Ford, A. C. and Murray, T. J. 1959. Studies on haemobartonella infection in the rat. *Can. J. Microbiol* **5**: 345–350. [Medline] [CrossRef]
4. Ford, W. W. and Eliot, C. P. 1928. The transfer of rat anemia to normal animals. *J. Exp. Med.* **48**: 475–492. [Medline] [CrossRef]
5. Fujita, H., Watanabe, Y. and Takada, N. 1995. Prevalence and properties of *Haemobartonella*-like microorganisms in field rodents in Fukushima Prefecture, Japan. *Jpn. J. Sanit. Zool.* **46**: 159–162.
6. Harasawa, R. 1996. PCR: application of nested PCR to detection of mycoplasmas. pp.75–79. *In*: Molecular and Diagnostic Procedures in Mycoplasmology, vol. 2 (Razin, S. and Tully, J. G. eds.), Academic Press, New York.
7. Harasawa, R. 1999. Genetic relationships among mycoplasmas based on the 16S-23S rRNA spacer sequence. *Microbiol. Immunol.* **43**: 127–132. [Medline]
8. Harasawa, R. and Kanamoto, Y. 1999. Differentiation of two biovars of *Ureaplasma urealyticum* based on the 16S-23S rRNA intergenic spacer region. *J. Clin. Microbiol.* **37**: 4135–4138. [Medline]
9. Harasawa, R., Hotzel, H. and Sachse, K. 2000. Comparison of the 16S-23S rRNA intergenic spacer regions among strains of the *Mycoplasma mycoides* cluster, and reassessment of the taxonomic position of *Mycoplasma* sp. bovine group 7. *Int. J. Syst. Evol. Microbiol.* **50**: 1325–1329. [Medline] [CrossRef]
10. Harasawa, R., Kawahara, M. and Rikihisa, Y. 2002. Characteristics of the 16S-23S rRNA intergenic spacer region of *Myco-*

plasma haemomuris, previously classified as '*Haemobartonella muris*'. *J. Vet. Med. Sci.* **64**: 1161–1164. [Medline] [CrossRef]
11. Harasawa, R., Pitcher, D. G., Ramirez, A. S. and Bradbury, J. M. 2004. A putative transposase gene in the 16S-23S rRNA intergenic spacer region of *Mycoplasma imitans*. *Microbiology* **150**: 1023–1029. [Medline] [CrossRef]
12. Harasawa, R., Uemori, T., Asada, K., Kato, I. and Shiragami, N. 1992. 'boxA'-like sequence between the 16S/23S spacer in the rRNA operon. *FEBS Lett.* **297**: 209–211. [Medline] [CrossRef]
13. Kessler, W. R. 1943. Studies on experimental *Bartonella muris* anemia in the albino rat. II. Latent infection and resistance. *J. Infect. Dis.* **73**: 77–84. [CrossRef]
14. Kimura, M. 1980. A simple method for estimating evolutionary rates of base substitutions through comparative studies of nucleotide sequences. *J. Mol. Evol.* **16**: 111–120. [Medline] [CrossRef]
15. Messick, J. B. 2004. Hemotrophic mycoplasmas (hemoplasmas): a review and new insights into pathogenic potential. *Vet. Clin. Pathol.* **33**: 2–13. [Medline] [CrossRef]
16. Neimark, H., Johansson, K. E., Rikihisa, Y. and Tully, J. G. 2001. Proposal to transfer some members of the genera *Haemobartonella* and *Eperythrozoon* to the genus *Mycoplasma* with the descriptions of '*Candidatus* Mycoplasma haemofelis', '*Candidatus* Mycoplasma haemomuris', '*Candidatus* Mycoplasma haemosuis' and '*Candidatus* Mycoplasma wenyonii'. *Int. J. Syst. Evol. Microbiol.* **51**: 891–899. [Medline] [CrossRef]
17. Neimark, H., Johansson, K. E., Rikihisa, Y. and Tully, J. G. 2002. Revision of haemotrophic mycoplasma species names. *Int. J. Syst. Evol. Microbiol.* **52**: 683. [Medline]
18. Noguchi, H. 1928. Etiology of Oroya fever. XI. Comparison of *Bartonella bacilliformis* and *Bartonella muris*. Cultivation of Bacterium murium, N. sp. *J. Exp. Med.* **47**: 235–243. [Medline] [CrossRef]
19. Rikihisa, Y., Kawahara, M., Wen, B., Kociba, G., Fuerst, P., Kawamori, F., Suto, C., Shibata, S. and Futohashi, M. 1997. Western immunoblot analysis of *Haemobartonella muris* and comparison of 16S rRNA gene sequences of *H. muris, H. felis*, and *Eperythrozoon suis*. *J. Clin. Microbiol.* **35**: 823–829. [Medline]
20. Saitou, N. and Nei, M. 1987. The neighbor-joining method: a new method for reconstructing phylogenetic trees. *Mol. Biol. Evol.* **4**: 406–425. [Medline]
21. Sasaoka, F., Suzuki, J., Fujihara, M., Watanabe, Y., Nagai, K. and Harasawa, R. 2012. Examination of the 16S-23S rRNA intergenic spacer sequences of '*Cadidatus* Mycoplasma haemobos' and *Mycoplasma haemofelis*. *J. Vet. Med. Sci.* **74**: 83–87. [Medline] [CrossRef]
22. Sasaoka, F., Suzuki, J., Watanabe, Y., Fujihara, M., Nagai, K., Hirata, T. and Harasawa, R. 2013. Two genotypes among '*Candidatus* Mycoplasma haemobos' strains based on the 16S-23S rRNA Intergenic spacer sequences. *J. Vet. Med. Sci.* **75**: (in press) [PMID: 23064449].
23. Schilling, V. 1929. Weitere beiträge zur *Bartonella muris ratti*, ihre übertragung auf weisse Mäuse und eine eigene *Bartonella muris musculi* N. sp. bei splenektomieten weissen Mäusen. *Klin. Wochenschr.* **8**: 55–58. [CrossRef]
24. Thompson, J. D., Higgins, D. G. and Gibson, T. J. 1994. CLUSTAL W: improving the sensitivity of progressive multiple sequence alignment through sequence weighting, position-specific gap penalties and weight matrix choice. *Nucleic Acids Res.* **22**: 4673–4680. [Medline] [CrossRef]
25. Volokhov, D. V., Simonyan, V., Davidson, M. K. and Chizhikov, V. E. 2012. RNA polymerase beta subunit (*rpoB*) gene and the 16S-23S rRNA intergenic transcribed spacer region (ITS) as complementary molecular markers in addition to the 16S rRNA gene for phylogenetic analysis and identification of the species of the family *Mycoplasmataceae*. *Mol. Phylogenet. Evol.* **62**: 515–528. [Medline] [CrossRef]
26. Zuker, M. and Stiegler, P. 1981. Optimal computer folding of large RNA sequences using thermodynamics and auxiliary. *Nucleic Acids Res.* **9**: 133–148. [Medline] [CrossRef]